



Insights into the Selective Inhibition of *Candida albicans* Secreted Aspartyl Protease: A Docking Analysis Study

S. K. Pranav Kumar and Vithal M. Kulkarni*

Pharmaceutical Division, Department of Chemical Technology, University of Mumbai, Mumbai 400 019, India

Received 23 August 2001; accepted 26 October 2001

Abstract—Severe fungal infections have taken precedence over other bacterial infections. Of the several fungal species, *Candida albicans* and others belonging to the genus *Candida* are responsible for several clinically important fungal infections. Emerging cases of drug resistance to the currently available drugs has limited the spectrum of currently available antifungal agents. Thus, it is imperative that new biochemical targets are identified so that better effective and selective agents can be developed. Many enzymes contribute towards the complex disease process of fungal infections; the secreted aspartyl protease (SAP), expressed both in vitro and during infection, has been implicated as one of the major virulence factors of *C. albicans*. Three-dimensional crystal structures of *C. albicans* SAP and closely related clinical isolate designated as SAP2X complexed with the same potent inhibitor **A-70450** have been reported. Several analogues of A-70450 with potent *C. albicans* SAP2X inhibitory activity are also known. However, the structural effects of the binding of these compounds with the enzyme active site are not completely understood. Our efforts in this direction involve the docking analysis of *C. albicans* SAP2X inhibitors complexed with SAP2X enzyme, which is reported in this work. Docking analysis was performed on a set of molecules with differing selectivities and inhibitory potencies towards *C. albicans*, renin and cathepsin D. The structural effects of ligand binding were analyzed on the basis of hydrophobic and hydrogen bond interactions, binding energy analysis, interaction energies, *rms* deviations, etc. in the resulting energy-minimized structures of the receptor–ligand complexes. Structural analysis of the resulting models indicates that hydrophobic and hydrogen bonding interactions together with binding and interaction energies are responsible for selective inhibition of *C. albicans* SAP2X. Hydrophobic and hydrogen bonding interactions in the various subsites of the enzyme, contributing to both increase as well as decrease in selectivity of the molecules have been detailed. Hydrogen bonding interaction plays an important role for amino acid residues such as Gly-85, Asp-86, Asp-32, Asp-218, Tyr-225, Ala-133, and so on. Significant hydrophobic interactions with the S₃, S₂ and S₂' subsites contribute to selectivity of the compounds. These molecular modeling analyses should, in our view, contribute for further development of selective *C. albicans* secreted aspartyl protease inhibitors. © 2002 Published by Elsevier Science Ltd.

Introduction

Fungal diseases until few years ago were considered of less importance with relation to bacterial and other parasitic infections.^{1–3} However, over the past two decades a alarming rise in life-threatening fungal infections of varying types and frequencies have been observed in immunocompromised patients. Patients with chemotherapy induced neutropenia and those receiving organ transplant-associated immunosuppressive therapy are highly susceptible to the life-threatening fungal infections. Other factors which have contributed to the rise in fungal infections include invasive medical procedures involving extensive surgery and/or use of prosthetic devices and vascular catheters, treatment regimes involv-

ing either broad spectrum antibiotics or glucocorticoids, peritoneal dialysis, hemodialysis and parenteral nutrition.^{4–6}

Fungal infections vary widely with respect to clinical picture and mainly include superficial mycoses involving infections to skin, hair, mucous membrane and nails. Deep mycoses are systemic infections, which are difficult to treat. Being eukaryotic organisms, fungi carry true nucleus, that is they possess chromosomes enclosed by nuclear membrane. This fact makes fungal infections difficult to treat without affecting the host organisms. The major opportunistic pathogen has been *Candida albicans*; however, the frequency of non-*C. albicans* *Candida* species is also increasing.^{4,7–10} This problem of increased fungal infections is accentuated by the emergence of fungal strains, which are resistant to currently used antifungal agents. Major opportunistic fungal pathogens include *Candida albicans*, *Aspergillus* sp., and

*Corresponding author. Tel.: +91-22-414-5616; fax: +91-22-414-5614; e-mail: vithal@biogate.com vmk@pharma.udct.ernet.in

Trichophyton mentagrophytes. Other species of *Candida* such as *C. krusei*, *C. tropicalis*, *C. glabrata* are major causative agents of candidiasis. HIV-infected patients are particularly susceptible to mucosal candidiasis, cryptococcal meningitis, disseminated histoplasmosis, and coccidioidomycosis. Clinically, candidosis and aspergillosis account for between 80 and 90% of systemic fungal infections in immunocompromised patients.

Although several azole antifungal agents are used in the treatment of a variety of mycotic infections, incidences of resistance to these currently available antifungals warrant the development of alternative therapies. Also, more importantly use of currently available azoles in combination with other antifungal agents with different mechanisms of action is likely to provide enhanced efficacy. In light of these developments, new antifungal agents with different mechanisms of action and broad-spectrum antifungal activities are needed for the effective management of these clinically important infections. One such target is the secreted aspartyl protease (SAP) from *C. albicans*, a putative factor responsible for virulence.¹¹

Because of their ubiquitous nature, the aspartic proteinases are involved in various commercial and biomedical processes.^{12,13} Examples of such proteinases are numerous, with the HIV virus being the well-known pathogen, which utilizes an aspartic proteinase in mediating critical aspects of its life cycle. Aspartic proteinase enzymes are also present in other disease-causing agents responsible for infectious processes. Enzymes belonging to the class of fungal aspartic-proteinases from *Rhizopus chinensis*,¹⁴ *Endothia parasitica*¹⁵ and *Penicillium janthinellum*¹⁶ have been well characterized which reveal the archetypical 'bilobal' fold associated with the proteinase family. These are mainly β structures which are organized into two domains consisting of an Asp-Thr-Gly (DTG)/Asp-Ser-Gly (DSG) motif in the center of the extended cleft.¹³ In comparison with the crystal structures of the above enzymes, the fungal aspartyl proteinases from the *Candida* family also exhibit the 'bilobal' fold but with substantial structural variations within the active site of the fungal proteinases. The general acid-base mechanism for the peptide hydrolysis catalyzed by the aspartic proteases is shown in Figure 1. The apostructures of the aspartic proteases exhibit the presence of a water molecule bound between the two aspartate residues, which is believed to be the nucleophile for the amide bond hydrolysis.¹³ The water molecule, in turn, is itself activated by a deprotonated catalytic aspartic acid residue. The protonated aspartic acid in turn donates a proton to the amide bond nitrogen resulting in a protonated nitrogen thereby generating the tetrahedral intermediate. The breakdown of the tetrahedral intermediate results in the formation of amide hydrolysis products.^{17–20}

Multiple interactions between *Candida* and the host determine the complex process of candidal infections with the secreted aspartic (acid) proteinases (SAPs) from *C. albicans*, *C. tropicalis*, *C. parapsilosis* and other fungal pathogens being implicated as virulence factors.^{11,21–24} These proteinases present unusually broad substrate specificity. The *Candida* strains express

at least seven distinct genes (SAPs 1–7) grouped into two subfamilies represented by SAPs 1–3, and SAPs 4–6, with SAP7 being the most divergent in sequence.²⁵ Thus, the SAP gene family plays an important role in the pathophysiology of *Candida*, exhibiting differential expressions during growth states, morphologic and phenotypic transitions, stages of infections and tissue sites during infection. Of the various SAP genes, SAP2 is the major form expressed in a number of strains under laboratory conditions on protein as the sole nitrogen source, which encodes a 398-residue pre-protein processed to a 342-residue mature enzyme with a deduced molecular mass of 35,880 Da.²⁶ SAP2 displays sensitivity towards pepstatin, which is a non-specific general inhibitor of aspartic proteases with a pH optimum between 3 and 4. It has also been shown that pepstatin can modulate the course of *C. albicans* infection in the mouse model,^{27,28} which further implicates SAP as a virulence factor. However, pepstatin because of its non-selectivity and lack of potency and safety is not an ideal agent for its use in therapy. It is active at neutral pH on appropriate substrates.²⁹ Also, regulation of SAPs by phenotypic switching^{30,31} and serum/hypha formation^{31,32} are representative of polymorphism and are particular properties of *C. albicans*, possibly contributing towards pathogenesis. Strong evidences for the involvement of proteinases in the fungal infection process come from the existence of correlations between virulence and level of protease expression, the low virulence and reduction in colonizing ability of protease-deficient mutants, detection of SAP and antibody to SAP in tissues and fluids of infected patients and the ability of SAP to degrade a broad range of substrates including proteins such as IgG heavy chains, keratin, acidified collagen and extracellular matrix proteins.^{11,21–24}

The three-dimensional structure of a close homologue of SAP2 (referred to as SAP2X) from *C. albicans* complexed with the potent inhibitor **A-70450** has provided considerable insight into the interactions of the ligand with the active site of the enzyme.³³ In addition, Cutfield and co-workers have reported the crystal structure of SAP2 complexed with two inhibitors—pepstatin and compound **A-70450**.³⁴ Also, Foundling and co-workers have reported the molecular structure of the secreted aspartic proteinase from *C. tropicalis* in complex with an unknown tetrapeptide tentatively identified as Thr-Ile-Thr-Ser (SAPT).³⁵ The crystal structure has also been successful in revealing the novel and subtle structural variations of the fungal proteinases over other classical aspartic proteinase enzymes. Structure–activity relationships of some of the analogues of compound **A-70450** have been reported.³³ However, in order to further probe into the selective interactions and binding modes of these analogues with the active site of *C. albicans* SAP2X and with our previous experience in the field of aspartic proteinases, we report herein a docking analysis study of the analogues of **A-70450** complexed with the active site of *C. albicans* SAP2X.

Molecular mechanics based methods involving docking studies and also molecular dynamics simulations have been used to study the binding orientations and prediction

of binding affinities. Such studies have been applied in case of plasmepsin II inhibitors,³⁶ *C. albicans* dihydrofolate reductase inhibitors,³⁷ interleukin-1 β converting enzyme (ICE) inhibitors,³⁸ human synovial fluid phospholipase-A₂ inhibitors,³⁹ non-peptidic inhibitors of HIV-1 protease⁴⁰ and matrix metalloproteinases (MMPs).⁴¹ Such studies have also been used to quantitatively predict the binding affinities as in the case of Herpes simplex virus thymidine kinase inhibitors.⁴²

Methodology

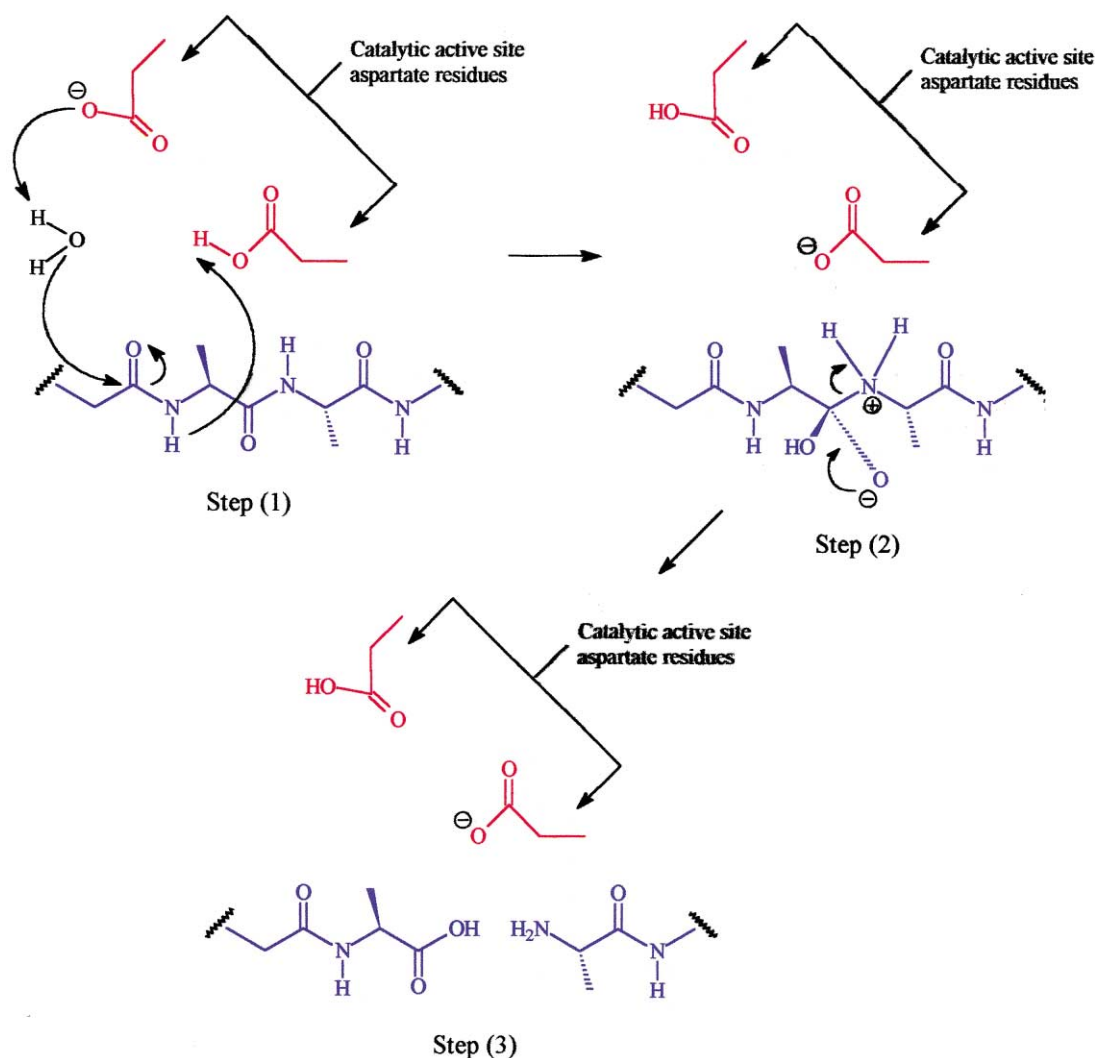
All calculations were performed on Silicon Graphics IRIS 4D/20 Personal Iris workstation (Silicon Graphics Inc., USA). CHARMM version 22 was used for all the molecular mechanics calculations and molecular

dynamics simulations. Model building, visualization and manipulation of the structures was performed using the molecular modeling package QUANTA.⁴³

Starting enzyme structure

The initial coordinates for the starting enzyme structure used in the model building process were those published for A-70450 complexed with *C. albicans* SAP2X (PDB entry 1zap)³³ obtained from the protein data bank, Brookhaven National Laboratory.⁴⁴ X-ray crystal structure served as a good starting model for the various inhibitors after a superposition exercise because of a good degree of similarity.

All the hydrogens were added to the enzyme structure. X-ray crystallographic water molecules associated with



- Step (1) : Nucleophilic attack of activated water molecule on the scissile amide bond resulting in protonation of the amide nitrogen
 Step (2) : Formation of the tetrahedral intermediate
 Step (3) : Amide hydrolysis products

Figure 1. Catalytic mechanism for aspartic proteinase mediated amide bond hydrolysis.

Table 1. Structures, activity data and selectivity indices of the compounds used in the docking analysis³³

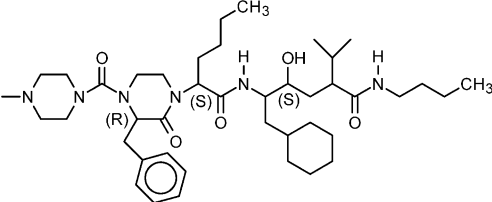
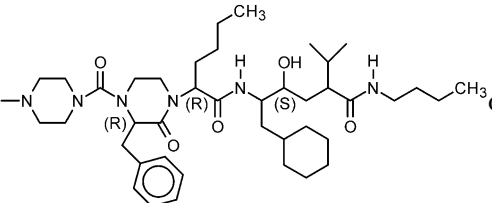
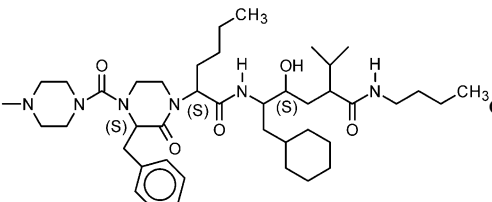
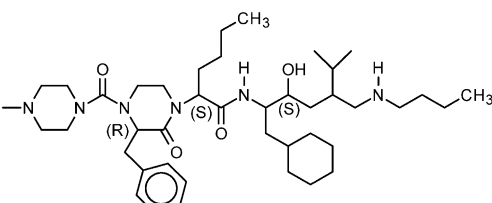
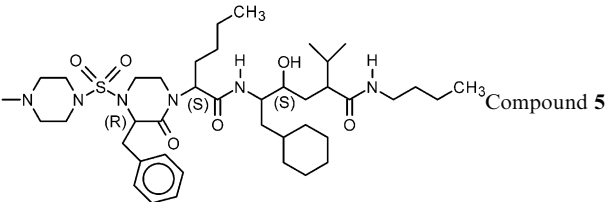
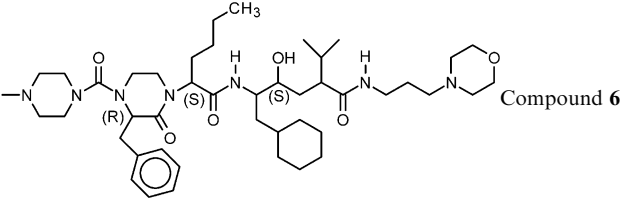
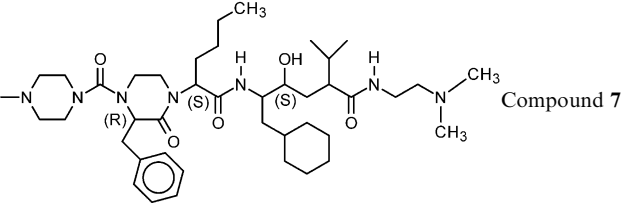
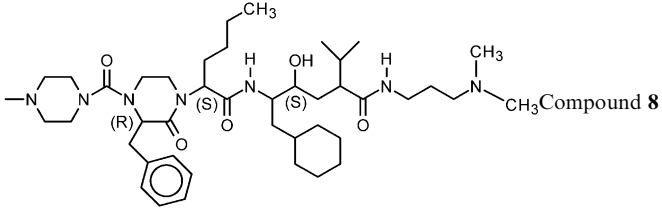
Structure of the compounds	IC ₅₀ (nM) against <i>C. albicans</i> ^a	IC ₅₀ (nM) against renin ^b	IC ₅₀ (nM) against Cat D ^c	Selectivity index ^d (renin)	Selectivity index ^d (Cat D)
 Compound A-70450	1.4	7.1	770	5.07	550
 Compound 2	25	na	na	—	—
 Compound 3	2.0	> 100	na	> 50	—
 Compound 4	490	na	na	—	—

Table 1 (continued)

Structure of the compounds	IC ₅₀ (nM) against <i>C. albicans</i> ^a	IC ₅₀ (nM) against renin ^b	IC ₅₀ (nM) against Cat D ^c	Selectivity index ^d (renin)	Selectivity index ^d (Cat D)
	2.7	1.5	150	0.55	55.55
	3.8	110	22,000	30	5800
	6.2	> 100	58,000	16.1	9354
	3.8	140	16,000	36.8	4210

^aIC₅₀ (nM) values for inhibition of *C. albicans*.^bIC₅₀ (nM) values for inhibition of renin.^cIC₅₀ (nM) values for inhibition of Cat D.^dSelectivity indices calculated by: S.I. = [IC₅₀ (nM) renin (or Cat D)/IC₅₀ (nM) *C. albicans*]. This value represents the amount by which the inhibitor is selective towards *C. albicans* over renin or Cat-D.

the *C. albicans* SAP2X/A-70450 complex were removed. In order to attenuate any internal strains in our model of *C. albicans* SAP2X at its current level of refinement (resolution = 2.7 Å), the well-documented multistage minimization procedure⁴⁵ was used in which atoms were unconstrained in stages to remove strained interactions. First the hydrogen atoms were energy minimized, with all other atoms fixed, and the α -carbon atoms of the model were constrained to remain as close as possible to the corresponding α -carbon atoms of the X-ray structure. Once the coordinates of all the atoms of the protein were computed, the entire molecule was subjected to energy minimization in which constraints of the α -carbon atoms were gradually removed. The energy of the whole complex was minimized until a convergence criterion of 0.001 kcal/mol/Å was achieved. Calculations were performed using the steepest descent and conjugate gradient minimization algorithms. The minimization was carried out in a continuum medium of relative permittivity $\epsilon = 4rij$.⁴⁶ The resulting structure subsequently served as the starting structure for further energy refinement, docking and complex formation.

Ligands

Structures and activities of the inhibitors (analogues of A-70450) against *C. albicans* SAP2X, renin and cathepsin D, employed in the current modeling study are given in Table 1. A preliminary structure activity relationship of these inhibitors with respect to the crystal structure of SAP2X complex has been made.³³ These analogues of A-70450 exhibit significant specificity towards *C. albicans* over renin and cathepsin D. Each of the ligands was built using the coordinates of A-70450 as it appears in the crystal structure, with standard bond lengths and angles within QUANTA, followed by energy minimization as described earlier using steepest descent and conjugate gradient minimization algorithms. Partial atomic charges were assigned to the enzyme and ligands by Gasteiger method. The protocol employed by Majer and co-workers⁴⁷ was used to modify the crystallographically bound inhibitor A-70450 wherein the side chains in the P₃, P₂, P₁, P₁' and P₂' positions were systematically mutated based on visual inspection of the binding site interactions. As each residue at different sites of the inhibitor was mutated, it was first optimized for steric interactions by manually manipulating the side chains so that the mutated side chain was able to occupy a maximum volume of the residue within the respective subsite of the enzyme as found in A-70450 and also to avoid close contacts with

the active site residues of the enzyme that would lead to unfavorable interaction energies. Energy minimization was then performed with the CHARMM force field as implemented in QUANTA molecular modeling package. In each case, the protein structure was held constant while the inhibitor was energy minimized in the protein cavity. Approximately 500 iterations of steepest descent was followed by conjugate gradient minimization until the gradient fell below 0.05 kcal/mol/Å or the difference between the successive energies was below 0.01 kcal/mol. Once the mutated ligands were generated from the crystallographically bound inhibitor A-70450, the inhibitors were removed from the active site of the enzyme and were subjected to systematic conformational search using 100 ps molecular dynamics simulations as previously reported at 300 K.³⁸ Dynamics were equilibrated for 10 ps with time step of 1 fs and continued for 100 ps simulations. The resulting low energy structure was extracted and energy minimized to 0.001 kcal/mol/Å. Non-bonded cutoff distance of 10 Å and a distance dependent dielectric constant ($\epsilon = 4rij$) was employed. All calculations were performed on a Silicon Graphics IRIS 4D/20 workstation (Silicon Graphics Inc., USA). CHARMM was used for all the molecular mechanics calculations and model building was performed using QUANTA molecular modeling software.

Docking procedure

To find sterically reasonable binding geometries for specific interactions of a ligand in the active site pocket of *C. albicans* SAP2X, the docking analysis was performed using QUANTA. The lowest potential energy conformers from molecular dynamics simulations were taken to be best candidates for the docking analysis. The conformers with probable hydrogen bonding were placed in the enzyme cavity by superposition of similar heteroatoms with those of the reference frame (crystal structure). The origin of this reference frame is situated in the active site pocket of *C. albicans* SAP2X. Employing interactive docking procedure, the ligands were docked into the enzyme active site by a random combination of translation, rotation, and torsional changes. This random move of the ligand samples both the orientational and conformational spaces of the ligand with respect to the enzyme active site. The orientation with low intermolecular potential energy was obtained by moving the ligand molecule slowly into the active site and updating the interaction energy continuously. The final minimized structure was accepted or rejected on the basis of energy and similarity criteria.

Table 2. Calculations of solvent accessible surface areas

Compound	Hydrophilic surface area	Hydrophobic surface area	Total solvent accessible surface area	Total enclosed volume
A-70450	96	961	1056	2132 ± 09
2	90	1054	1144	2222 ± 16
3	87	1039	1125	2232 ± 14
4	81	983	1065	2140 ± 15
5	113	993	1105	2229 ± 14
6	112	1026	1139	2317 ± 18
7	105	976	1080	2187 ± 03
8	101	1011	1112	2250 ± 18

Structure similarity was checked by calculating the *rms* deviations of the ligand between the current structure and structures found so far. After docking, the complex structure was energy minimized by applying constraints to hydrogen bonded atoms in the active site. Finally, the whole system was relaxed to low *rms* value by using conjugate gradient method.

Surface area calculations

Total solvent accessible surface areas together with hydrophilic and hydrophobic surface areas were calculated as implemented within QUANTA. The results are summarized in Table 2. Solvent accessible surface area calculations indicate that the non-polar surface areas of all the SAP2X inhibitor molecules are higher than the polar surface area. Since the active site surface area of SAP2X is high, the active site of this enzyme demands ligands, which possess more hydrophobic character.

Results

Various methods are known to dock a conformationally flexible ligand into the active site of protein. The algorithms involved in these methods use different techniques such as molecular dynamics, metropolis Monte Carlo, Monte Carlo minimization, genetic algorithms, distance geometry, and tree searching to explore the conformational space of the ligand and enzyme during docking calculations.⁴⁸ A docking calculation should be able to produce a crystal geometry of the ligand/enzyme complex with reasonable accuracy. Successful docking of the ligand would depend on the optimum choice of the variables involved in docking calculations. The conformational flexibility of each enzyme and ligand could be different for each particular type of ligand/enzyme complexes. Thus, in order to elucidate the binding modes of compound **A-70450** and its analogues as inhibitors of *C. albicans* SAP2X with better specificity over renin and cathepsin D, docking analysis was performed wherein the enzyme/inhibitor models of the inhibitors complexed with *C. albicans* SAP2X were generated.

All the compounds were constructed using standard geometry and standard bond lengths. A systematic conformational search of all the compounds was performed using 100 ps molecular dynamics simulations as previously reported at 300 K.³⁸ Dynamics were equilibrated for 10 ps with time step of 1 fs and continued for 100 ps simulations. The resulting low energy structure was extracted and energy minimized to 0.001 Kcal/mol/Å, which were further employed for docking and model generation.

Based on the three-dimensional crystal structure of SAP2X complexed with compound **A-70450**, a retrospective investigation and some generalizations regarding the structure–activity relationships of analogues of compound **A-70450**⁴⁹ has been made. However, a detailed computational analysis, which provides insights into the structural aspects mediating the inhibition of *C. albicans* SAP2X, would be of significance when design-

ing novel non-peptidic inhibitors of SAP2X enzyme. Towards this end, we have made an effort to correlate the structural factors responsible for SAP2X inhibition.

Analysis of the enzyme/ligand complex models generated after successful docking of the inhibitors was based on the following parameters:

- Hydrogen bond interactions
- Interactions such as π – π stacking interactions and hydrophobic interactions
- Energy of binding $E_{\text{binding}} = E_{\text{complex}} - (E_{\text{enzyme}} + E_{\text{compound}})$
- rms* deviation of active site residues
- Orientation of the inhibitor within the active site

As a general rule, in most of the aspartic proteinases where the inhibition of the enzyme is brought about by inhibitor ligands, specific hydrogen bond and hydrophobic interactions between the inhibitor main chain and the active site subsites of the enzyme have been found to be responsible for mediating protease inhibition. Taking into consideration these factors, we have used hydrogen bond and hydrophobic interactions as the major criterion for analysis.

Energy of binding was calculated for each compound, after minimization of the enzyme/inhibitor complex model, as the difference between the energy of the complex and individual energies of the enzyme and the ligand:

$$E_{\text{binding}} = E_{\text{complex}} - (E_{\text{enzyme}} + E_{\text{compound}})$$

Interaction of each ligand with the *C. albicans* SAP2X enzyme was compared on the basis of interaction energy of each ligand with the non-conserved amino acid residues of the active site. Thus, the interaction of each ligand with the non-conserved amino acid residues of SAP2X should govern the ability of that ligand to selectively inhibit the aspartyl protease. Differences in these interaction energies reflect the differences in the SAP2X inhibitory potency and selectivity of the ligands.

Dynamics followed by molecular docking were performed on each of the ligand under consideration. All the compounds in the current study differ with respect to the configuration of the substituent at either or both of the P_{3a} and P₂ sites of the inhibitor. Variations in most of the structures in the current series of analogues of **A-70450** occur only at the P₂' site of the inhibitor with rest of the molecule being unchanged. The orientation for each compound discussed here represents the best orientation and is a representative of all possible interactions within the active site of the SAP2X enzyme.

Compound A-70450

Compound **A-70450** was originally prepared as a part of renin inhibition program⁵⁰ by Abbott Laboratories which was later discovered to inhibit the SAP of *C. albicans*.⁴⁹ It is the most potent inhibitor with an IC₅₀

(nM) value of 1.4 (Table 1). On the selectivity index (S.I.), it has a value of 5.07 over renin and a value of 550 over Cathepsin D (Cat D). Although the compound lies in an extended conformation in the active site, it presents a unique branched structure at P_3 position of the inhibitor. The S_3 subsite of SAP2X is unusual due to its large size and has been operationally divided into two sections— S_{3a} and S_{3b} .³³ While the methylpiperazine group occupies the S_{3b} binding site of the enzyme, the P_{3a} benzylic substituent of the ketopiperazine ring occupies the S_{3a} subsite and exhibits *R*-configuration although for typical linear aspartyl protease inhibitors, the optimal configuration at this position is *S*-configuration. This change in configuration occurs due to the cyclization of the P_3 unit into a ketopiperazine ring thereby forcing the α -amino group of the P_3 unit into a different position than observed for acyclic inhibitors.³⁴ Docking analysis reveals that the side chains of S_{3a} subsite amino acid residues Val-12, Ile-30 and Ile-223 make hydrophobic interactions with benzylic substituent at P_{3a} site of the inhibitor. The side chains of Thr-221 and Thr-222 also interact with the inhibitor at this subsite of the enzyme. Similarly, the methylpiperazine moiety interacts with the S_{3b} subsite amino acid residues Tyr-51, Asp-86, and Asp-120. The *n*-butyl (nor-leucine unit) at P_2 , which exhibits *S*-configuration, extends and interacts into the S_2 subsite of the enzyme. The side chains of the amino acid residues Thr-221, Tyr-225, Asn-300, Ala-302 and Ile-304 make strong hydrophobic and van der Waals interactions with the *n*-butyl substituent. The cyclohexylmethyl substituent at P_1 site

of the inhibitor extends into the S_1 subsite and also exhibits *S*-configuration. This hydrophobic substituent interacts with the hydrophobic side chains of the amino acid residues including Ile-30, Tyr-84, Ser-88, Ile-119 and Ile-123. Interactions are also observed with the residues Gly-85, Gly-220 and Thr-221. The isopropyl substituent at P_1' in *S*-configuration interacts favorably with S_1' subsite making hydrophobic contacts with the side chains of the amino acid residues Leu-216 and Ile-304. The amidic side chains of Asn-131 and Glu-193 also interact favorably with the isopropyl substituent. Interactions are also observed with Gly-34 and Gly-85. The butyl substituent at P_2' of the inhibitor extends into the S_2' subsite making hydrophobic and van der Waals contacts with Gly-34, Ser-35, Ser-36, Asp-37, Ile-82, Gly-83 and Tyr-84. The side chains of the amino acid residues Asn-131, Glu-132 and Ala-133 also contribute towards interactions with the inhibitor side chain at this subsite of the enzyme.

Compound **A-70450** forms eight stable hydrogen bonds with the active site of the enzyme (H-bonding distance <3.00 Å). The binding orientation of compound **A-70450** is depicted in Figure 2. –NH of Gly-85 forms hydrogen bond interactions with the inhibitor P_1' (107.43°; 2.57 Å) (1) and P_2 (125.38°; 2.71 Å) (2) carbonyl moieties. –NH of Asp-86 and –NH of Thr-222 also form hydrogen bonds with the P_2 (139.16°; 2.59 Å) (3) and P_{3a} (156.18°; 2.40 Å) (4) ketopiperazine carbonyl functionalities of the inhibitor, respectively. The hydroxyl moiety of the hydroxyethylene peptide bond

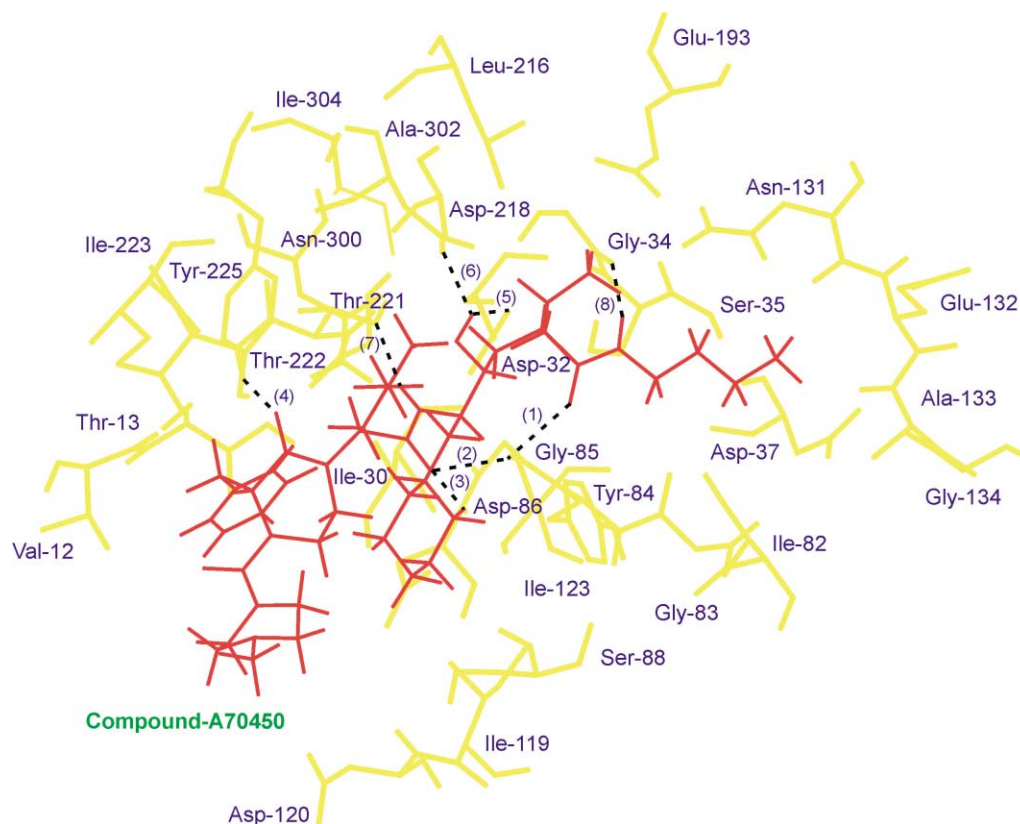


Figure 2. Binding orientation of compound **A-70450** within the active site of *C. albicans* SAP2X. Active site amino acid residues (within 4 Å from the inhibitor) are displayed in yellow while the inhibitor is displayed in red color. Hydrogen atoms of the enzyme have been suppressed for the purpose of clarity. Figures in parentheses correspond to the hydrogen bond distances (refer to text).

isostere which serves as a transition-state mimic interacts, in its *S*-configuration, forming hydrogen bonds with the catalytically active aspartate residues Asp-32 (120.13°; 2.72 Å) (5) and Asp-218 (160.07°; 2.13 Å) (6). The hydroxyl group of Thr-221 and the carbonyl moiety of Gly-34 both accept a hydrogen bond each from the –NH at P₂ (139.17°; 2.11 Å) (7) and –NH at P₂' (161.51°; 2.12 Å) (8) of the inhibitor main chain, respectively. These interactions result in a favorable orientation of the compound within the active site with energy of binding of –106.22 kcal/mol.

These hydrophobic interactions coupled with specific hydrogen bonding interactions especially with the catalytically active aspartate residues, confer the compound with maximum activity towards *C. albicans* SAP2X. However, though the compound is highly active towards SAP2X, specificity is low when compared to its analogues.

Compound 2

Compound **2** is essentially similar to the earlier one, the only change being made at the P₂ *n*-butyl (nor-leucine unit) side chain wherein the *S*-configuration is switched to *R*-configuration, that is compound **2** is epimeric to compound **1**. This change results in a significant drop in the potency of the compound, which inhibits SAP2X with IC₅₀ (nM) value of 25. Thus, the *S*-configuration at P₂ of the inhibitor is significantly crucial to maintain specific hydrophobic and van der Waals contacts with

the S₂ subsite amino acid residues of the enzyme. The changes are reflected, more specifically, in the inability of the *n*-butyl side chain to make favorable hydrophobic and van der Waals interactions with the S₂ subsite amino acid residues including Gly-85, Tyr-225, Asn-300, Ala-302 and Ile-304. The *R*-configuration of the *n*-butyl at P₂ results in the side chain being oriented towards S_{3a} pocket; thus interactions with S_{3a} binding pocket residues including Thr-221, Thr-222 and Ile-223 are observed. Moreover, the S₂ binding pocket is smaller and hence fails to accommodate the isomeric structure. Because of the restrictions placed at this site, substituents only in their *S*-configuration are tolerated.

As a result of this configurational switch, the favorable interactions of benzylic substituent at S_{3a} pocket with the amino acid residues Val-12, Ile-30, Thr-222, Ile-223 and Gly-220 are lost. Moreover, the methylpiperazine also exhibits diminished interactions with S_{3b} pocket residues including Tyr-51, Asp-86, and Asp-120. These changes account for the decrease in inhibitory potency. The configuration switch alters the binding pattern of the inhibitor and also mediates changes in subsites distal to S₂ pocket. As a result, the P₁ cyclohexylmethyl substituent fails to interact with Ser-88 and Gly-220 at S₁ subsite as also the S₁' isopropyl which fails to interact with Thr-221 and Ile-304. Other interactions are however preserved to a large extent, which confers the compound with some degree of inhibitory activity towards SAP2X.

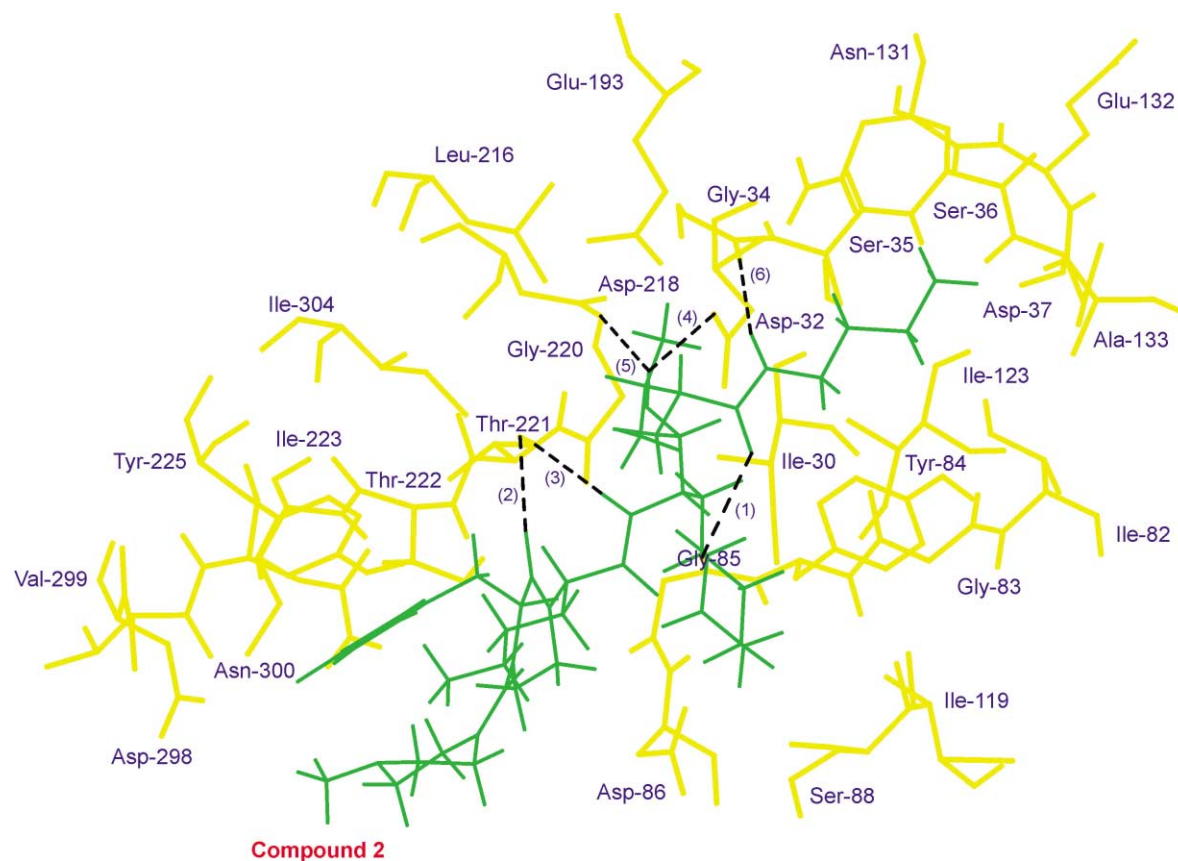


Figure 3. Binding orientation of compound **2** within the active site of *C. albicans* SAP2X. Active site amino acid residues (within 4 Å from the inhibitor) are displayed in yellow while the inhibitor is displayed in green color. Hydrogen atoms of the enzyme have been suppressed for the purpose of clarity. Figures in parentheses correspond to the hydrogen bond distances (refer to text).

Compound **2** forms six hydrogen bonds, with energy of binding -95.77 kcal/mol. The binding orientation of compound **2** is depicted in Figure 3. As earlier, the $-\text{NH}$ of Gly-85 forms a hydrogen bond with the inhibitor P_1' (111.17° ; 2.61 Å) (1) carbonyl moiety. The hydroxyl of Thr-221 acts both as a donor and acceptor forming a very weak hydrogen bond with carbonyl of ketopiperazine moiety at P_3a (97.90° ; 2.76 Å) (2) and a strong hydrogen bond with $-\text{NH}$ at P_2 (168.18° ; 2.15 Å) (3) of the inhibitor main chain. The hydroxyl of the hydroxyethylene isostere forms hydrogen bond interactions with Asp-32 (122.98° ; 2.68 Å) (4) and Asp-218 (139.09° ; 2.09 Å) (5). The carbonyl of Gly-34 accepts a hydrogen bond from the $-\text{NH}$ at P_2' (162.85° ; 2.06 Å) (6) of the inhibitor main chain. Thus, the overall changes in both hydrophobic as well as specific hydrogen bond interactions, mediated as a result of change in the binding orientation of the compound, makes it less inhibitory towards SAP2X.

Compound 3

Compound **3** is similar to compound **2**, with a configuration switch being made from (*R*) \rightarrow (*S*) to the benzylic substituent of the ketopiperazine moiety at P_3a site of the inhibitor. This configuration is opposite to that found in compound **A-20470**. Unlike compound **2**, the *S*-configuration at P_2 *n*-butyl (nor-leucine unit) substituent as in compound **1** is preserved. Thus compound **3** is also epimeric to compound **1**. However, compound **3** preserves its inhibitory potency unlike compound **2**,

where a configuration switch about the P_2 substituent results in significant drop in inhibitory potency. Compound **3** inhibits SAP2X with a IC_{50} (nM) value of 2.0. Interestingly, the selectivity towards SAP2X is enhanced to >50 -fold over renin, thus indicating the preference of *S*-configuration of the benzylic substituent at S_3a subsite of the enzyme. The *S*-configuration in this analogue contributes towards greater selectivity towards SAP2X whereas an *R*-configuration (as in compound **1**) contributes towards enhanced inhibitory potency of the compound. This preference can be rationalized by the favorable interactions of the compound at this subsite. The benzylic substituent exhibits strong hydrophobic and π - π stacking interactions with the side chains of Ile-223 and Tyr-225. Interactions are also observed with the side chains of Gly-220, Thr-221, Thr-222 and Asp-86 amino acid residues. These interactions are favorable from a selectivity point of view. Similarly, the methylpiperazine interacts with the S_3b subsite and makes favorable interactions with the side chains of amino acid residues Tyr-51, Asp-86, Ser-88 and Asp-120. Thus, the compound retains the inhibitory potency as in compound **1** which is reflective of the ability of the S_3 binding pocket to accommodate isomeric structures. Interactions of *n*-butyl and cyclohexymethyl substituents with S_2 and S_1 subsites of the enzyme, respectively, are essentially similar to that of compound **1**. In addition to its interactions as in compound **1**, the isopropyl substituent at P_1' also interacts with the side chain of Thr-221. Interactions of the butyl substituent with S_2' of the enzyme remain similar to that of

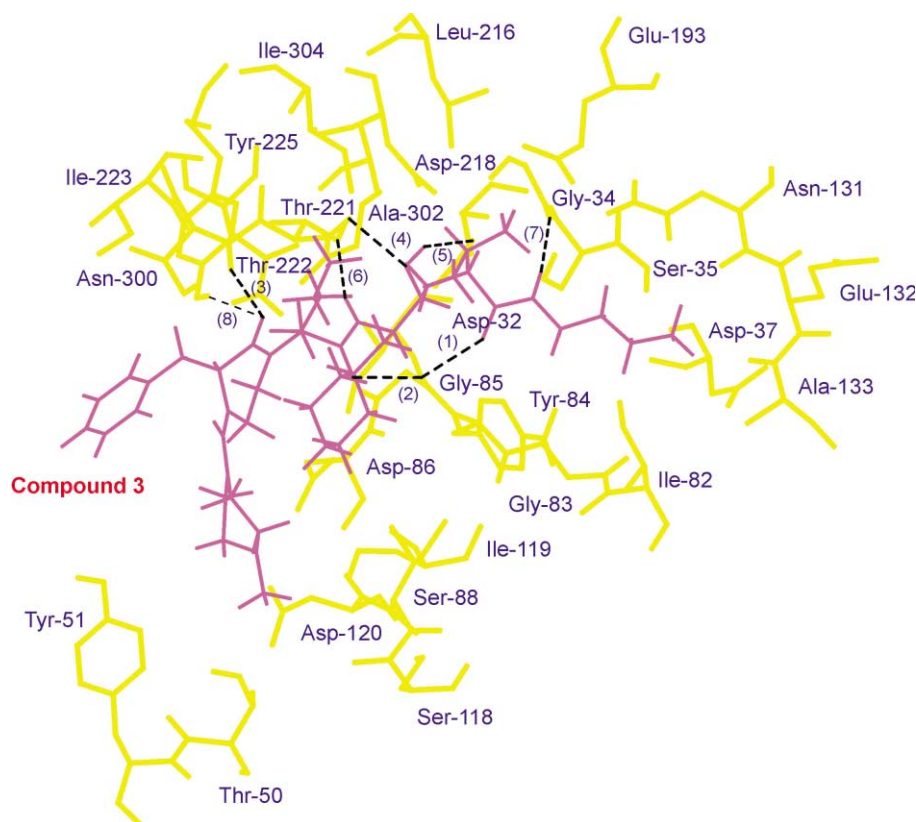


Figure 4. Binding orientation of compound **3** within the active site of *C. albicans* SAP2X. Active site amino acid residues (within 4 Å from the inhibitor) are displayed in yellow while the inhibitor is displayed in magenta color. Hydrogen atoms of the enzyme have been suppressed for the purpose of clarity. Figures in parentheses correspond to the hydrogen bond distances (refer to text).

compound **1**. The binding orientation of compound **3** is depicted in Figure 4.

Compound **3** forms eight good hydrogen bonds, with energy of binding -99.83 kcal/mol. $-NH$ of Gly-85 forms hydrogen bond interactions with the inhibitor P_1' (105.46° ; 2.66 Å) (1) and P_2 (123.96° ; 2.59 Å) (2) carbonyl moieties. Similarly, the $-NH$ of Thr-222 forms hydrogen bond with the P_{3a} (152.43° ; 2.23 Å) (3) ketopiperazine carbonyl functionality of the inhibitor. The hydroxyl moiety of hydroxyethylene isostere at P_1 , forms hydrogen bonds with $-NH$ of Thr-221 (100.52° ; 2.00 Å) (4) and Asp-32 (127.46° ; 2.45 Å) (5). The hydroxyl group of Thr-221 and the carbonyl moiety of Gly-34 both accept a hydrogen bond each from the $-NH$ at P_2 (145.29° ; 2.06 Å) (6) and $-NH$ at P_2' (162.85° ; 2.06 Å) (7) of the inhibitor main chain, respectively. A hydrogen bond is also formed between the hydroxyl group of Tyr-225 and the carbonyl functionality of the ketopiperazine moiety at P_{3a} of the inhibitor (156.69° ; 2.60 Å) (8). It is a well-known fact that strong interactions of catalytically active aspartate residues with the centrally located hydroxyl moiety of the peptide bond isostere is one of the major driving forces contributing towards the inhibitory efficacies and also to some extent towards the selectivity of aspartyl protease inhibitors. The observed decrease in the strength of these crucial hydrogen bonds (with Thr-221 and Asp-32) probably contributes to the slightly reduced inhibitory potency of this compound. However, the hydrogen bond interaction with the Tyr-225 residue contributes towards specificity of the compound. Thus, specific hydrophobic and van der Waals contacts of the inhibitor with the subsites of the enzyme active site coupled with selective hydrogen bond interactions confer selectivity to the compound albeit with a corresponding reduction in its inhibitory potency.

Compound 4

Compound **4** retains the (*R*)- and (*S*)-configurations of the benzylic substituent of ketopiperazine at P_{3a} and *n*-butyl (nor-leucine unit) substituent at P_2 , respectively. However, this compound represents a reduced-bond analogue of compound **1** at the $P_1'-P_2'$ linkage. The absence of a carbonyl functionality at this linkage greatly reduces the inhibitory potency of the compound, since in compound **1**, the carbonyl moiety acts as a hydrogen bond acceptor forming a hydrogen bond with the $-NH$ of Gly-85 residue. Compound **4** inhibits SAP2X with a IC_{50} (nM) value of 490. Thus, the carbonyl moiety serves not only as recognition point for interacting with the active site amino acid residues but also contributes strongly towards the inhibitory potency of the compound. Since the hydrogen bond is lost, the inhibitor binds in a orientation different from that of compound **1** within the active site, with a corresponding shift in the backbone atoms of the enzyme. The hydrophobic and van der Waals interactions are however maintained at the respective subsites of the enzyme, with changes being reflected mainly in the interactions of the P_1' isopropyl substituent with the S_1' subsite. The change in orientation and conformation of the inhibitor results in the isopropyl substituent making interactions

with the S_{3a} subsite residue Thr-221. Interactions of the butyl substituent with S_2' of the enzyme remain similar to that of compound **1**.

Prominent changes are, however, observed in the hydrogen-bonding pattern rather than hydrophobic interactions, which presumably account for the significant drop in potency of this compound. Compound **4** forms seven hydrogen bonds with energy of binding -103.40 kcal/mol. $-NH$ of Gly-85, which normally forms a hydrogen bond with the P_1' carbonyl functionality, now forms a strong hydrogen bond with P_2 (138.94° ; 2.33 Å) carbonyl of the inhibitor. Formation of this strong hydrogen bond prevents the proper alignment of the inhibitor within the active site. The $-NH$ of Asp-86 and $-NH$ of Thr-222, as earlier, form hydrogen bonds albeit weaker ones, with the P_2 (119.02° ; 2.45 Å) and P_{3a} (121.49° ; 2.39 Å) ketopiperazine carbonyl functionalities of the inhibitor, respectively. The hydroxyl moiety of hydroxyethylene isostere at P_1 forms significantly weak hydrogen bonds with $-NH$ of Thr-221 (99.23° ; 2.54 Å) and Asp-32 (109.35° ; 2.83 Å). Hydrogen bond interactions with Thr-221 and Gly-34 are preserved with the hydroxyl group of Thr-221 and the carbonyl moiety of Gly-34 both accepting a hydrogen bond each from the $-NH$ at P_2 (140.07° ; 2.05 Å) and $-NH$ at P_2' (128.71° ; 2.10 Å) of the inhibitor main chain, respectively.

Thus, the subtle changes in hydrogen bonding pattern together with changes in hydrophobic interactions and inhibitor orientation within the active site of the enzyme, as described above explain the significant drop in potency of this compound.

Compound 5

Compound **5** is similar to compound **1**, wherein a sulfonyl linkage between the P_{3a} ketopiperazine and P_{3b} methylpiperazine of the inhibitor replaces the urea carbonyl of compound **1**. The configurations of the substituents at P_{3a} and P_2 of are similar to compound **1** and hence not much variation in the inhibitory potency of the compound is observed. Also the linkage, either urea carbonyl or sulfonyl, does not interact with the active site amino acid residues. Compound **5** inhibits *C. albicans* SAP2X with a IC_{50} (nM) value of 2.7. Compound **5** has an S.I. value of 0.55 over renin (not significant) and a value of 55.55 over Cat D.

The sulfonyl linkage between the P_{3a} and the P_{3b} substituents at the S_3 subsite of the enzyme results in rigidification of the linkage, thereby altering the conformation of the P_{3b} methylpiperazine ring and its interactions with the corresponding active site amino acid residues; interactions are observed only with Tyr-51. The hydrophobic and van der Waals interactions of the substituents at other subsites of the enzyme remain similar to that observed for compound **1**.

Compound **5** forms eight hydrogen bonds with energy of binding -99.75 kcal/mol. However, change in conformation of the P_{3b} fragment due to the sulfonyl linkage

results in alterations of the hydrogen-bonding pattern. The carbonyl of this fragment moves away from the optimum hydrogen-bonding distance with Tyr-225 residue. This change is reflected in the loss of a hydrogen bond between the hydroxyl of Tyr-225 and the carbonyl functionality of the S_{3a} ketopiperazine moiety. Other hydrogen bond interactions mediated by Gly-85, Asp-86, Thr-221, Thr-222, the catalytically active Asp-32 and Asp-218 and Gly-34 are essentially similar to those observed in compound **1** although somewhat weaker bonds ensue. Thus, loss of hydrogen bond with Tyr-225 together with changes in other hydrogen bonding interactions complemented by subtle changes in hydrophobic interactions presumably contribute to the observed decrease in selectivity of this compound over renin (more prominent) and cathepsin D.

Compound 6

Compound **6** is similar to compound **1**, with modifications being made only at P₂' of the inhibitor wherein a morpholine ring replaces one of the methyl group in the butyl chain. This replacement has a significant effect on the selectivity of the compound although the inhibitory potency is compromised. The (*R*)- and (*S*)-configurations of the P_{3a} and the P₂ substituents, respectively, are preserved as in compound **1**. Compound **6** inhibits SAP2X with a IC₅₀ (nM) value of 3.8. It exhibits a significantly high S.I. of ~30 towards SAP2X over renin and a S.I. of ~5800 over Cat D. This high selectivity of compound **6** over both renin and Cat D probably stems from additional interactions contributed by the changes made at P₂' side chain of the inhibitor.

Docking analysis reveals that the P_{3a} substituent exhibits significant interactions with the side chains of the S_{3a} subsite amino acid residues including Val-12, Ile-30, Thr-222 and Ile-223. Similarly, the methylpiperazine moiety interacts with the S_{3b} subsite amino acid residues Tyr-51, Asp-86, and Asp-120. At S₂ subsite, the P₂ *n*-butyl (nor-leucine unit) exhibits strong hydrophobic and van der Waals interactions with the side chains of amino acid residues including Thr-221, Tyr-225, Asn-300, Ala-302 and Ile-304. On a similar line as compared to compound **1**, the P₁ cyclohexylmethyl substituent extends into the S₁ binding pocket and interacts with the hydrophobic side chains of Ile-30, Tyr-84, Ser-88, Ile-119 and Ile-123. Interactions are also observed with the residues Gly-85, Gly-220 and Thr-221. The side chains of Gly-34, Gly-85, Glu-193, Leu-216 and Ile-304 interact with the P₁' isopropyl substituent within the S₁' subsite of the enzyme. At P₂' of the inhibitor a morpholine ring replaces one of methyl group in the butyl side chain in compound **1**. Although one would think of additional interactions because of this change, docking analysis indicates that both the morpholine ring and the butyl side chain occupy essentially the same space and exhibit interactions with the same S₂' binding pocket residues. However, it is the hydrogen bond interactions, which contribute towards the high selectivity of this compound. The morpholine ring extends into the S₂' binding pocket and makes hydrophobic and van der Waals contacts with the active site residues including

Gly-34, Ser-35, Ser-36, Asp-37, Ile-82, Gly-83 and Tyr-84. The side chains of the amino acid residues Asn-131, Glu-132 and Ala-133 also contribute towards interactions with the inhibitor side chain.

Compound **6** forms 10 stable hydrogen bonds with the active site of the enzyme. –NH of Gly-85 forms hydrogen bond interactions with the inhibitor P₁' (113.79°; 2.16 Å) and P₂ (126.44°; 2.79 Å) carbonyl moieties. –NH of Asp-86 and –NH of Thr-222 also form hydrogen bonds with the P₂ (139.02°; 2.51 Å) carbonyl and P_{3a} (147.72°; 2.52 Å) ketopiperazine carbonyl functionality of the inhibitor, respectively. The hydroxyl moiety of the hydroxyethylene peptide bond isostere forms a very weak hydrogen bond with –NH of Thr-221 (95.56°; 2.62 Å) and another with Asp-32 (132.42°; 2.56 Å). The hydroxyl of Tyr-225 forms a strong hydrogen bond with the carbonyl functionality of the ketopiperazine moiety at P_{3a} of the inhibitor (158.93°; 2.55 Å). The hydroxyl group of Thr-221 and the carbonyl moiety of Gly-34 both accept a hydrogen bond each from the –NH at P₂ (137.10°; 2.13 Å) and –NH at P₂' (152.67°; 2.44 Å) of the inhibitor main chain, respectively. In addition to these interactions, the oxygen atom of the morpholine ring results in the formation of a strong hydrogen bond with the donor –NH of Ala-133 (137.44°; 2.28 Å). This additional hydrogen bond together with the hydrogen bond contributed by Tyr-225 enables the compound to exhibit significantly high selectivity towards SAP2X enzyme. From the above results, it appears that Tyr-225 residue acts as a specific recognition element in determining the selectivity of SAP2X inhibitors. These interactions result in a favorable orientation of the compound within the active site with energy of binding of –108.14 kcal/mol. However, the observed decrease in inhibitory potency can be ascribed to the loss in hydrogen bond interactions of the inhibitor with Asp-218 and the weak hydrogen bond interactions with Asp-32 and Thr-221.

Compound 7

Compound **7** is similar to compound **6** except that a dimethyl aminoethyl side chain occupies the P₂' site of the inhibitor. This replacement further enhances the selectivity of the compound over renin as well as Cat D, although a further drop in inhibitory potency is observed when compared to compound **6**. This drop in potency is however largely compensated by the very high selectivity of this compound towards SAP2X over Cat D. Compound **7** inhibits SAP2X with an IC₅₀ (nM) value of 6.2. It exhibits a nominal S.I. of ~16 towards SAP2X over renin and an extremely high S.I. of >9000 over Cat D. This high selectivity of compound **7** over Cat D probably arises from the presence of an branched aliphatic substituent at P₂' of the inhibitor.

Docking analysis of compound **7** reveals a similar pattern of hydrophobic and van der Waals interactions at various subsites of the enzyme as in compound **6**. However, when compared to other substituents at P₂', the branched dimethyl aminoethyl substituent at this site is able to extend deep into the S₂' subsite and make

strong interactions with the active site amino acid residues. This is reflected in better interactions being mediated by the residues Ser-35, Ser-36, Asp-37, Asn-131 and Gly-134 with the P_2' substituent. Interactions with other residues remain similar to compound **6**. The binding orientation of compound **7** is depicted in Figure 5.

Compound **7** forms nine hydrogen bonds with energy of binding -121.63 kcal/mol. However, it is the 'strength' and pattern of these hydrogen bonds, which differentiate the selectivity pattern and inhibitory potency of one compound over the other. The $-NH$ of Gly-85 forms a strong hydrogen bond with P_2 (139.92° ; 2.48 Å) (1) carbonyl of the inhibitor. However, the presence of other stabilizing interactions helps maintain a proper alignment of the inhibitor so that optimum contacts and interactions at the respective subsites of the enzyme are preserved. Interactions of Asp-86 (2) and Thr-222 (3) are similar as in the earlier compound. Strong hydrogen bonds are formed between the hydroxyl moiety of the hydroxyethylene isostere and the catalytically active aspartate residues Asp-32 (132.16° ; 2.52 Å) (4) and Asp-218 (149.92° ; 2.12 Å) (5). The hydroxyl also forms a hydrogen bond with $-NH$ of Thr-221 (115.95° ; 2.73 Å) (6). The hydroxyl of Tyr-225 forms a strong hydrogen bond with the carbonyl functionality of the ketopiperazine moiety at P_{3a} of the inhibitor (163.64° ; 2.51 Å) (7). Similarly, strong hydrogen bond interactions are observed with Thr-221 and Gly-34 residues. The hydroxyl group of Thr-221 and the carbonyl moiety of

Gly-34 both accept a hydrogen bond each from the $-NH$ at P_2 (149.87° ; 2.07 Å) (8) and $-NH$ at P_2' (153.82° ; 2.07 Å) (9) of the inhibitor main chain, respectively. Thus, the strong hydrogen bond interactions mediated by the residues Gly-85, Thr-221, the aspartate residues and Gly-34 together with favorable hydrophobic and van der Waals interactions at S_2' subsite contribute to the high selectivity of this compound towards SAP2X.

Compound 8

Compound **8** is also similar to compound **7** wherein a dimethyl aminopropyl side chain occupies the P_2' site of the inhibitor. This change in the P_2' substituent significantly reduces the selectivity of the compound towards Cat D and results in a slight improvement over renin selectivity. However, the inhibitory potency of the compound is restored, comparable to that of compound **6**. Compound **8** inhibits SAP2X with an IC_{50} (nM) value of 3.8 . It exhibits an S.I. of ~ 37 towards SAP2X over renin and a significantly high S.I. of > 4000 over Cat D.

Docking analysis of compound **8** reveals no changes in active site residue interactions with the P_2' site where the variation in the side chain is made, indicating the ability of this site to accommodate various substituents. Thus, the hydrophobic and van der Waals interactions of the substituents from P_3 to P_2' with the subsites S_3 to S_2' remain essentially similar to those observed in case of compound **7**.

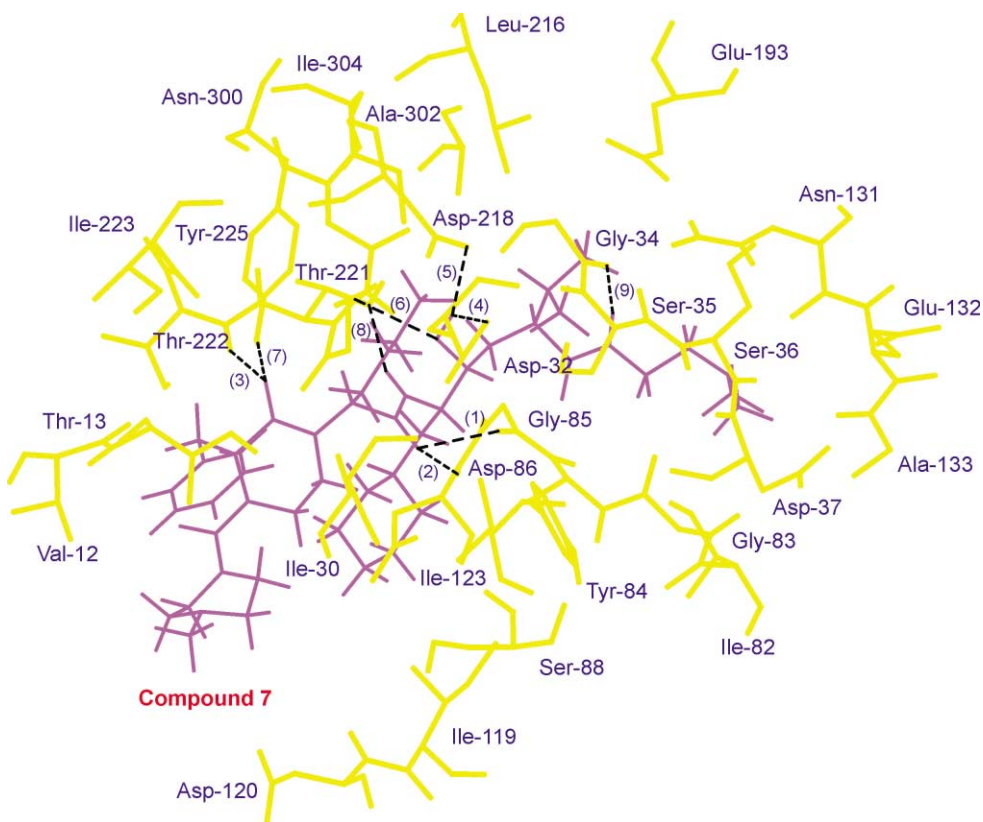


Figure 5. Binding orientation of compound **7** within the active site of *C. albicans* SAP2X. Active site amino acid residues (within 4 Å from the inhibitor) are displayed in yellow while the inhibitor is displayed in purple color. Hydrogen atoms of the enzyme have been suppressed for the purpose of clarity. Figures in parentheses correspond to the hydrogen bond distances (refer to text).

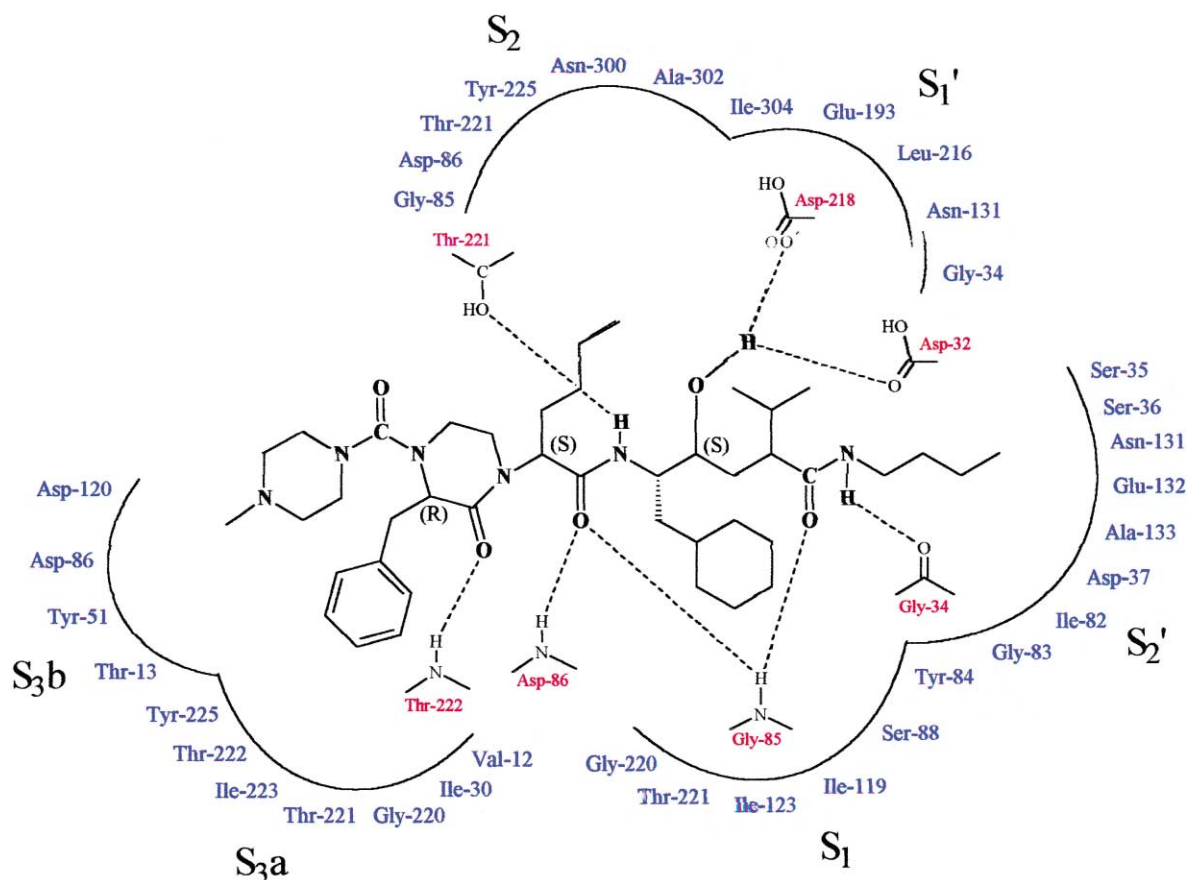


Figure 6. Schematic representation of the interactions of compound **A-70450** with the active site of *C. albicans* SAP2X.

Extension of the P_2' substituent by one carbon atom, however, results in a slight conformational change of the inhibitor so that the orientation of the inhibitor is altered, resulting in subtle variations in hydrogen bond interactions. Compound **8** forms nine hydrogen bonds with energy of binding -114.39 kcal/mol. Unlike compound **7**, the $-NH$ of Gly-85 forms hydrogen bonds with the inhibitor P_1' (109.86° ; 2.56 Å) and P_2 (125.01° ; 2.55 Å) carbonyl moieties. $-NH$ of Asp-86 and $-NH$ of Thr-222 also form hydrogen bonds with the P_2 (139.14° ; 2.40 Å) carbonyl and P_{3a} (149.52° ; 2.51 Å) ketopiperazine carbonyl functionality of the inhibitor, respectively. The hydroxyl moiety of the hydroxyethylene peptide bond isostere forms a very weak hydrogen bond with $-NH$ of Thr-221 (96.33° ; 2.83 Å) and another with Asp-32 (125.54° ; 2.63 Å). The hydroxyl of Tyr-225 forms a strong hydrogen bond with the carbonyl functionality of the ketopiperazine moiety at P_{3a} of the inhibitor (155.90° ; 2.74 Å). The hydroxyl group of Thr-221 and the carbonyl moiety of Gly-34 both accept a hydrogen bond each from the $-NH$ at P_2 (141.54° ; 2.11 Å) and $-NH$ at P_2' (174.56° ; 2.07 Å) of the inhibitor main chain, respectively. The interactions are similar to that of compound **6**, which help preserve the inhibitory potency of compound **8**. However, the near-4-fold reduction in selectivity of this compound towards Cat D can be related to the absence of a hydrogen bond with Ala-133 (as found in compound **6**) and loss of optimal hydrophobic interactions and van der Waals contacts with the S_2' subsite residues (as in compound **7**) due to

the extension of P_2' side chain by a single carbon atom. These interactions together with other hydrogen bonding parameters retain the inhibitory potency of the compound but result in a significant drop in selectivity of the compound.

Discussion

The extracellular proteolytic activity of *C. albicans* is mediated by the aspartyl protease enzymes.⁵¹ The activity of this secreted aspartyl proteinase was first described by Staib^{52,53} and over the last 25 years its role as a virulence factor has been the topic of significant research interest. Furthermore, three-dimensional structures of SAP2 and a closely related clinical isolate (referred to as SAP2X and also employed in the current docking analysis) of the SAP2, complexed with the same inhibitor **A-70450** have been reported.

The current study involving molecular dynamics and subsequent docking analysis of *C. albicans* SAP2X inhibitors (analogues of compound **A-70450**) has resulted in a new insight into the various structural factors and interactions responsible for the selectivity and inhibitory potency of SAP2X inhibitors. Schematic diagram of the interactions of compound **A-70450** with the active site of the *C. albicans* SAP2X enzyme is depicted in Figure 6. The binding elements (P_3 – P_2') have been labeled using the Schechter and Berger nomenclature

for proteases.⁵⁴ Molecular recognition and subsequent interactions of these inhibitors with the active site residues occur mainly through hydrogen bonding, hydrophobic and electrostatic contributions. Specific hydrogen bond interactions act not only as anchoring points for the inhibitors but also contribute towards specificity and inhibitory potency of these inhibitors. Also, the binding affinities of the inhibitors are influenced mainly by hydrogen bonding and hydrophobic interactions with the active site residues of the enzyme.

Compound **A-70450**, originally reported as renin inhibitor (as a part of Abbott renin inhibition program)⁵⁰ was later discovered to inhibit *C. albicans* SAP2X.⁴⁹ This compound is a pseudo-hexapeptide possessing hydroxyethylene peptide bond isostere with the hydroxy group located between the catalytically active aspartate residues Asp-32 and Asp-218. The lactam ring present in this compound (and its analogues) severely restricts the conformation around P₃, with the benzyl side chain of P₃ exhibiting the (*R*)-configuration. As a result, compound **A-70450** exhibits a curved backbone due to the lack of flexibility imposed by the lactam ring. This is in contrast to pepstatin generally employed to study the crystallographic characteristics of aspartic proteinase–inhibitor complexes, which exhibits an extended conformation. Pepstatin incorporates a central statine residue containing a non-scissile bond $-(\text{CHOH}-\text{CH}_2)-$ which acts as a tetrahedral transition-state mimic. Another interesting feature of compound **A-70450** and its analogues used in the current study is the conformation adapted by the substituents at P₃ and P₁. The benzylic substituent on the ketopiperazine moiety at P_{3a} of the inhibitors is equivalent to that of D-phenylalanine, which by virtue of its flexibility mediates intermolecular interactions with the P₁ cyclohexyl substituent, which folds towards the P_{3a} site occupied by the benzylic substituent. This is consistent with the crystal structure of **A-70450** complexed with *C. albicans* SAP.³⁴

Compound **A-70450** is the most potent inhibitor with an IC₅₀ (nM) value of 1.4, followed by compounds **3**, **5**, **6** (**8**) and **7** with IC₅₀ (nM) values of 2.0, 2.7, 3.8 (3.8) and 6.2, respectively. Compounds **6** and **8** have similar IC₅₀ (nM) values. Hydrophobic and van der Waals interactions together with hydrogen bonding interactions (wherein the ‘strength’ of the H-bond is an important criteria) of the substituents with the subsites of the enzyme determine the selectivity and inhibitor potency of this series of compounds. The benzyl group of the ketopiperazine moiety occupies the S_{3a} subsite and makes interactions with the S_{3a} subsite residues Val-12, Ile-30, Thr-221, Thr-222 and Ile-223. Similarly, the methylpiperazine moiety at S_{3b} exhibits interactions with Tyr-51, Asp-86, and Asp-120. Compound **3** is isomeric to compound **1**, with the benzylic side chain of the ketopiperazine moiety in the (*S*)-configuration. This isomeric change, however, does not alter the inhibitory capacity, but interestingly enhances the selectivity of the compound by a factor of > 50 towards SAP2X over renin. On one hand, this property of ability of incorporation of isomeric structures at the S₃ subsite is due to the large S₃ binding pocket and on the other hand,

enhancement of selectivity occurs due to favorable interactions with the S₃ subsite residues. The *n*-butyl (nor-leucine unit) substituent of all the inhibitors at P₂, which exhibits *S*-configuration, interacts with the S₂ subsite binding pocket making hydrophobic and van der Waals contacts with the residues including Thr-221, Tyr-225, Asn-300, Ala-302 and Ile-304. These residues help stabilize the *n*-butyl substituent. However, in compound **2** where the *n*-butyl substituent exhibits (*R*)-configuration, these interactions are lost with a corresponding reduction in the activity of the compound. This occurs as a result of the smaller and more restrictive S₂ binding pocket, which is unable to accommodate the isomeric structures. Thus, substituents with only (*S*)-configuration are tolerated at this subsite.

The cyclohexylmethyl substituent at P₁, in its (*S*)-configuration interacts with the S₁ subsite residues including Ile-30, Tyr-84, Ser-88, Ile-119 and Ile-123. Interactions are also observed with the residues Gly-85, Gly-220 and Thr-221. Residues Ile-119 and Ile-123, which are involved in defining the inhibitor-binding pockets, have also been observed in case of *C. albicans* SAP.³⁴ The isopropyl substituent at P₁ interacts favorably with S₁’ subsite making hydrophobic contacts with the side chains of the amino acid residues Gly-34, Gly-85, Asn-131, Glu-193, Leu-216 and Ile-304.

The P₂’ substituent occupying the S₂’ subsite of the enzyme has been modified in most of the analogues to confer selectivity on the inhibitor. However, hydrophobic and van der Waals contacts with Gly-34, Ser-35, Ser-36, Asp-37, Ile-82, Gly-83, Tyr-84, Asn-131, Glu-132 and Ala-133 are observed in almost all the inhibitors. Ile-82 and Tyr-84 residues form a part of the ‘flap’ and strong interactions with these flap residues is thought to stabilize enzyme–inhibitor interactions. In case of compound **6**, the formation of a single hydrogen bond between the P₂’ substituent and the active site alanine residue significantly enhances the selectivity of the compound over both renin and Cat D. However, the presence of a branched substituent as in compound **7** greatly enhances the selectivity parameter over renin and Cat D. Thus, the presence of an P_{3a} substituent in its (*S*)-configuration over the conventional (*R*)-configuration together with a branched substituent at P₂’ can be expected to result in a inhibitor with significantly high selectivity over both renin and Cat D, although no compound incorporating these features has been reported. These changes when brought about in the molecule can also be expected to possibly bring about highly conducive changes in the hydrogen bonding pattern which can further enhance not only selectivity but also the inhibitory potency of the compound. The docking analysis of the individual compounds supports this assumption.

As a general rule, although the analogues differ in structures to each other, similar interactions are preserved to a large extent and that the differences in activities and selectivities of the compounds occur mainly due to subtle changes in either optimal or sub-optimal filling of the active site binding pockets by the

Table 3. Binding orientation data for inhibitors with Plasmepsin-II enzyme

Compound	$E_{\text{bind}}^{\text{a}}$	$E_{\text{interNC}}^{\text{b}}$	H-bonds ^c
A-70450	−106.22	−50.04	8
2	−95.77	−35.06	6
3	−99.83	−38.79	8
4	−103.40	−36.27	7
5	−99.75	−37.72	8
6	−108.14	−46.15	10
7	−121.63	−64.55	9
8	−114.39	−58.37	9

^a E_{bind} is energy of binding calculated by $E_{\text{complex}} - (E_{\text{enzyme}} + E_{\text{inhibitor}})$ (kcal/mol).

^b E_{interNC} is interaction energy between the compound and non-conserved amino acid residues of active site.

^cH-bonds is the number of hydrogen bonds formed between the inhibitor and active site residues of the enzyme.

conformationally legal inhibitor side chains, which ultimately determine the strength of the enzyme–inhibitor interactions.

Apart from the strong hydrophobic and van der Waals contacts of the active site residues with the substituents at the respective subsites of the inhibitors, it is the ‘strength’ of the hydrogen bond interactions, which determine the inhibitory potencies, and more importantly the selectivity of the compounds in the present series of compounds. Although similar hydrogen bond interactions are observed in most of the analogues, variations in the ‘strength’ (a property related to the angle and distance of the hydrogen bond formed between the inhibitor and the enzyme) of the hydrogen bond interactions mediate selectivity and inhibitory potency. In case of SAP2X, the active site residues involved in hydrogen bond interactions include catalytically active Asp-32 and Gly-34 from one loop of the enzyme and Asp-218, Gly-220, Thr-221, Thr-222 and Tyr-225 from the other loop together with the flap residues Gly-85 and Asp-86. The involvement of these residues represents a common theme of interaction of aspartyl protease inhibitors with the active site of proteinase enzymes since these residues are highly conserved amongst the fungal members. Thus, the loss of hydrogen bond formation with the flap residue Gly-85 as in the case of compound **2**, results in a significant reduction of activity of the compound. This supports the crucial role of flap residues in stabilizing the ‘flap’ after binding of the inhibitor within the active site. The reduction in activity of this compound is also due to the formation of a weak hydrogen bond with Thr-221 and loss of hydrogen bond interaction with the flap residue Asp-86. In case of compound **3**, again a loss in hydrogen bond with Asp-86 accounts for the reduction in inhibitory potency of the compound. However, the involvement of the hydroxyl group of Tyr-225 in a strong hydrogen bond interaction accounts for the improved selectivity towards SAP2X over renin. The low level of selectivity of compound **A-70450** over other analogues in the series can be ascribed to the inability of this compound to exhibit hydrogen bond interactions with the hydroxyl group of Tyr-225, which probably acts as a recognition point in mediating the selectivity of this class of compounds.

Compound **4**, which represents a reduced bond between the P₁′ and P₂′ linkage, exhibits the lowest inhibitory potency. This is due to the inability of the inhibitor to form a hydrogen bond interaction with the flap residue Gly-85 at P₁′ of the inhibitor. Also, weak hydrogen bonds are observed with the active site residues Asp-32 and Asp-86. The high selectivity of compound **6** towards SAP2X over Cat D occurs mainly as a result of the presence of a morpholine ring at the P₂′ site of the inhibitor. The oxygen atom of this morpholine ring forms a strong hydrogen bond interaction with the S₂′ residue Ala-133. In addition to other conserved hydrogen bonds, the formation of this hydrogen bond together with a strong hydrogen bond mediated through the Tyr-255 residue results in the enhanced selectivity of compound **6**. The branched substituent at P₂′ in case of compound **7** is extremely conducive for the very high selectivity observed towards SAP2X over Cat D. This occurs as a result of strong hydrogen bond interactions with the flap residues Gly-34 and Gly-85. These interactions are further complemented by strong hydrogen bond interactions between the hydroxyl of the hydroxyethylene peptide bond isostere and the catalytic aspartate residues Asp-32 and Asp-218.

Analysis of binding energies of the compounds indicates that compounds possessing better selectivity profile exhibit high binding energies (Table 3). Compound **7**, which exhibits the highest selectivity towards SAP2X over Cat D, has a favorable binding energy of −121.63 kcal/mol. Also the interaction of the compound with the non-conserved residues of the enzyme has a value of −64.55 kcal/mol. These energies are observed as a result of favorable hydrophobic and hydrogen bonding interactions of the compound with the active site residues of the enzyme. Thus, the favorable interaction of these selective compounds is reflected in their binding energy values. Reduction in the interaction energies are observed in case of compounds with low selectivity profile and reduced inhibitory potency. For example, compound **4**, which is inactive towards SAP2X, has interaction energy of −36.27 kcal/mol.

Structural effects of ligand binding were analyzed from *rms* deviations between the non-hydrogen atoms of SAP2X and the inhibitors in the resulting energy-minimized structures of the SAP2X/inhibitor complexes compared to the starting structure of the receptor used in all simulations.

Binding of these inhibitors within the active site of SAP2X does not result in a large movement of the active site residues to accommodate the compounds. The patterns of *rms* deviations produced by the inhibitor binding in the complex are similar for all the inhibitor molecules and are in the range of 0.28–0.42 Å. The *rms* deviations of the C α positions with respect to the starting structure are all in the range of 0.23–0.36 Å, whereas the *rms* deviations of the backbone and the active site residues are in the range of 0.25–0.32 and 0.16–0.24 Å, respectively. *Rms* deviations for the inhibitors are in the range of 0.18–0.72 Å (Table 4), indicating that the inhibitors do not undergo much

Table 4. rms Deviations data for Pm-II enzyme and inhibitors

Compound	rmsd (enzyme) ^a	rmsd (inhibitor) ^b
A-70450	0.27	0.18
2	0.31	0.53
3	0.25	0.72
4	0.32	0.38
5	0.26	0.40
6	0.27	0.38
7	0.28	0.47
8	0.29	0.40

^armsd is the rms deviation of active site backbone as compared to the refined crystal structure.

^brmsd is the deviation between the non-hydrogen atoms of the ligand after energy minimization with that of the crystal structure.

distortion but that the minor deviations observed translate into the changes observed in the hydrogen bonding pattern made by the inhibitors with the active site of the enzyme. This suggests that the compounds with varying inhibitory potencies and/or selectivities bind to the active site of the enzyme with only subtle changes in their conformations. In general, it is observed that the hydrogen and hydrophobic interactions mainly contribute towards the activity of SAP2X inhibitors. The active site is able to accommodate the various substituents without inducing large movements within the active site of the enzyme. In summary, the nature of the active site residues and their effect on the binding conformations of the inhibitors influence the inhibitory potency and selectivity of these inhibitors.

The present study was performed on a selected set of compound with different inhibitory potencies and selectivity indexes. Although the compounds are similar to one another and are analogues of compound **A-70450**, due to some specific interactions with the enzyme, different energy terms or parameters such as binding energy, hydrophobic and electrostatic interactions and hydrogen bonding interactions were calculated and analyzed. It has been observed that in the present set of analogous compounds, some specific parameters are responsible for favorable interaction of specific compounds with the enzyme and, hence, different energy terms or parameters explain the selectivity of the compounds. However, major factors contributing to the selectivity of the present series of compound include binding energy, hydrophobic effects and specific hydrogen bonding interactions. Results from the present study are informative in a qualitative manner. The present study does not make any attempt to quantitate the results. Such a quantitative study would require a larger set of compounds and an accurate modeling protocol. It is also not a part of this study to include any common scoring function for comparison of various energy terms and a quantitative equation correlating these terms with biological activity.

To this extent, not many modeling studies concerning computational aspects of *C. albicans* secreted aspartyl protease have been reported to date. The present study is unique in the sense that the interactions responsible for the selective inhibition of SAP2X have been made. The study also attempts to understand the structural

factors responsible for the potency and selectivity of SAP2X inhibitors. Potency and selectivity of inhibitors have an important role during clinical application and thus the results from this selectivity analysis can be extrapolated for the design and synthesis of selective non-peptidic SAP2X inhibitors. The selectivity parameters considered during the design and synthesis of non-peptidic inhibitors may also help reduce side effects to the human host. Thus, finally, the results drawn from the present study should contribute towards development of potent and selective inhibitors of the secreted aspartyl protease from *C. albicans*.

Acknowledgement

The authors thank the University Grants Commission (UGC), New Delhi for the financial support under its COSIST program.

References and Notes

- Walsh, T. J.; Hiemenz, J. W.; Anaissie, E. *Infect. Dis. Clin. North Am.* **1996**, *10*, 365.
- Groll, A. H. *J. Infect.* **1996**, *33*, 23.
- Minamoto, G. Y.; Rosenberg, A. S. *Med. Clin. North Am.* **1997**, *81*, 381.
- Beck-Sague, C. M.; Jarvis, W. R. *Infect. Dis.* **1993**, *167*, 1247.
- Denning, D. W. *J. Antimicrob. Chemother.* **28**, (Suppl. B), 1.
- Diamond, R. D. *Rev. Infect. Dis.* **1991**, *13*, 480.
- Banerjee, S. N.; Emori, T. G.; Culver, D. H.; Gaynes, R. P.; Jarvis, W. R.; Horan, T.; Edwards, J. R.; Tolson, J.; Henderson, T.; Marone, W. J. *Nat. Nosocomial Infect. Surveillance Syst.* **1989**, *91*, 86.
- Kiehn, T. E.; Edwards, F. F.; Armstrong, D. *Am. J. Clin. Pathol.* **1980**, *73*, 515.
- Richardson, M. D. *Antimicrob. Agents Chemother.* **1991**, *28*, 1.
- Walsh, T. J.; Pizzo, P. A. *Ann. Rev. Microbiol.* **1988**, *42*, 517.
- Douglas, L. J. *Crit. Rev. Biotechnol.* **1988**, *8*, 121.
- Kostka, V., Ed. *Aspartic Proteinases and their Inhibitors*. Walter de Gruyter: Berlin, 1985.
- Davies, D. R. *Annu. Rev. Biophys. Biophys. Chem.* **1990**, *19*, 189.
- Subramanian, E. I. D. A.S.; Lie, M.; Davies, D. R.; Jenkins, J. A.; Tickle, I. J.; Blundell, T. L. *Proc. Natl. Acad. Sci. U.S.A.* **1977**, *74*, 556.
- Tang, J.; James, M. N. G.; Hsu, I. N.; Jenkins, J. A.; Blundell, T. L. *Nature* **1978**, *271*, 618.
- Hsu, I.; Delbaere, L. T. J.; James, M. N. G.; Hoffmann, T. *Nature* **1977**, *266*, 140.
- Fruton, J. S. *Adv. Enzymol. Relat. Areas Mol. Biol.* **1976**, *44*, 1.
- Dunn, B. M. *Adv. Detailed React. Mech.* **1992**, *2*, 213.
- Suguna, K.; Padlan, E. A.; Smith, C. W.; Carlson, W. D.; Davies, D. R. *Proc. Natl. Acad. Sci. U.S.A.* **1987**, *84*, 7009.
- James, M. N. G.; Sielecki, A. R.; Hayakawa, K.; Gelb, M. H. *Biochemistry* **1992**, *31*, 3872.
- Ray, T. L.; Payne, C. D.; Morrow, B. J. In *Aspartic Proteinase Conference on Structure and Function of the Aspartic Proteinases: Genetics, Structures, and Mechanisms*; Dunn, B. M. Ed.; Plenum: Sonoma County, CA, USA, 1990; p 173.
- Cutler, E. *Ann. Rev. Microb.* **1991**, *45*, 187.

23. Ruchel, R.; de Bernardis, F.; Ray, T. L.; Sullivan, P. A.; Cole, G. T. *J. Med. Vet. Mycol.* **1992**, *30*, 123.
24. White, T. C.; Kohler, G. A.; Miyadake, S. H.; Agabian, N. *Can. J. Botany* **1995**, *73* (Suppl. 1), 1058.
25. Monod, M.; Togni, G.; Hube, B.; Sanglard, D. *Mol. Microbiol.* **1994**, *13*, 357.
26. Wright, R. J.; Carne, A.; Hieber, A. D.; Lamont, I. L.; Emerson, G. W.; Sullivan, P. A. *J. Bacteriol.* **1992**, *174*, 7848.
27. Ruchel, R.; Ritter, B.; Schaffrinski, M. *Int. J. Med. Microbiol.* **1990**, *273*, 391.
28. Zotter, C.; Hausteiner, U. F.; Schonborn, C.; Grimmecke, H. D.; Wand, H. *Dermatol. Monatsschr.* **1990**, *176*, 189.
29. Wagner, T.; Borg-v Zepelin, M.; Ruchel, R. *J. Med. Vet. Mycol.* **1995**, *284*, 72.
30. White, T. C.; Miyasaka, S. H.; Agabian, N. *J. Bacteriol.* **1993**, *175*, 6126.
31. White, T. C.; Agabian, N. *J. Bacteriol.* **1995**, *177*, 5215.
32. Hube, B.; Monod, M.; Schofield, D. A.; Brown, A. J.; Gow, N. A. *Mol. Microbiol.* **1994**, *14*, 87.
33. Abad-Zapatero, C.; Goldman, R.; Muchmore, S. W.; Hutchins, C.; Stewart, K.; Navaza, J.; Payne, C. D.; Ray, T. L. *Protein Sci.* **1996**, *5*, 640.
34. Cutfield, S. M.; Dobson, E. J.; Anderson, B. F.; Moody, P. C. E.; Marshall, C. J.; Sullivan, P. A.; Cutfield, J. F. *Structure* **1995**, *3*, 1261.
35. Symersky, J.; Monod, M.; Foundling, S. I. *Biochemistry* **1997**, *36*, 12700.
36. Pranav Kumar, S. K.; Kulkarni, V. M. *Drug Des. Dis. In press*.
37. Gokhale, V. M.; Kulkarni, V. M. *J. Comput.-Aided Mol. Des.* **2000**, *14*, 495.
38. Hariprasad, V.; Kulkarni, V. M. *J. Mol. Model.* **1997**, *3*, 443.
39. Hariprasad, V.; Kulkarni, V. M. *J. Mol. Recogn.* **1996**, *9*, 95.
40. Hariprasad, V.; Talele, T. T.; Kulkarni, V. M. *Pharm. Pharmacol. Commun.* **1998**, *4*, 365.
41. Kiyama, R.; Tamura, Y.; Watanabe, F.; Tsuzuki, H.; Ohtani, M.; Yodo, M. *J. Med. Chem.* **1999**, *42*, 1723.
42. Winter, H. D.; Herdewijn, P. *J. Med. Chem.* **1996**, *39*, 4727.
43. QUANTA; Molecular Simulations Inc.: 9685, Scranton Road, San Diego, CA 92121-3752, USA.
44. Abola, E. E.; Bernstein, F. C.; Bryant, S. H.; Koetzle, T. F.; Weng, J.; Allen, F. H.; Bergerhoff, G.; Sievers, R., Eds. *Crystallographic Databases—Information Content, Software Systems, Scientific Applications*. Data Commission of International Union of Crystallography: Cambridge, UK, 1987.
45. Levit, M.; Lifson, S. *J. Mol. Biol.* **1969**, *46*, 269.
46. Orozco, M.; Laughton, C. A.; Herzyk, P.; Neidle, S. *J. Biomol. Struct. Dyn.* **1990**, *8*, 359.
47. Majer, P.; Collins, J. R.; Gulnik, S. V.; Erickson, J. W. *Protein Sci.* **1997**, *6*, 1458.
48. Cherfils, J.; Janin, J. *Curr. Opin. Struct. Biol.* **1993**, *3*, 265.
49. Goldman, R. C.; Baker, W. R.; Jae, H. S.; De, B.; Zydowsky, T. M.; de Lara, E. US Patent No. 5,120,718, 1991, to Abbott Laboratories.
50. De, B.; Zydowsky, T. N.; Baker, W. R.; Dellaria, J. F.; Rosenberg, S. H.; Jae, H. S. US Patent No. 5,164,388, 1991, to Abbott Laboratories.
51. Odds, F. C. In *Candida and Candidosis*, 2nd ed.; Bailliere Tindall: London, UK, 1988.
52. Staib, F. *Sabouraudia* **1965**, *4*, 187.
53. Staib, F. *Mycopathol. Mycol. Appl.* **1969**, *37*, 345.
54. Schechter, I.; Berger, A. *Biochem. Biophys. Res. Commun.* **1967**, *27*, 157.